Journal of GeoEngineering, Vol. 15, No. 1, pp. 55-68, March 2020
http://dx.doi.org/10.6310/jog.202003_15(1).5

A STUDY OF DYNAMIC SHEAR MODULUS AND BREAKAGE OF DECOMPOSED VOLCANIC SOILS

Ismail Adeniyi Okewale [1*] and Hennie Grobler [2]

ABSTRACT

Small strain shear modulus, G_{max}, is considered as a fundamental stiffness property for the soils and it is very important material parameter in design and analysis of geotechnical structures. It is also very important to estimate the particle breakage and its effects on mechanical properties required in engineering design. In this work, small strain shear modulus and breakage of five different volcanic soils were investigated in the reconstituted state. Reconstituted soil is common in the construction of geotechnical structures and their behaviour at very small strain is of utmost significance. This was achieved by conducting bender elements testing in triaxial stress path cells on uniformly graded volcanic soils. The particle breakage was estimated and analysed based on total energy input. The decomposed volcanic soils have weaker and crushable particles. The G_{max} increases with particle breakage which in turn increases with total energy input. A new model equation has been proposed for the estimation of G_{max} of volcanic soils. The small strain shear modulus is accurately predicted using empirical equation proposed for sand but the accuracy of prediction depends on the coarse fraction of the soil.

Key words: Small strain, shear modulus, particle breakage, shape descriptors, grading descriptors, volcanic soil.

1. INTRODUCTION

Detailed investigation into the behaviour of weathered geomaterials is very essential due to adverse effect of weathering processes on them and the consequent problems (*e.g.,* landslide) caused to engineering structures and men. One of the important aspects of the behaviour is the deformation characteristics at very small strain denoted by small strain shear modulus studied using bender elements or resonant column tests. Many investigations have been carried out on the small strain shear modulus usually represented as G_{max} of soils (*e.g.,* Gasparre *et al.* 2014; Jamiolkowski *et al.* 1991; Senetakis *et al.* 2012; Vagianni and Atkinson 1995; Hardin and Richart 1963). This can be attributed to significant role played by the small strain shear modulus in the design and analysis of engineering structures under different loadings as well as being taking as fundamental stiffness property.

However, very few of such studies were on weathered soils and the studies were much more limited for weathered volcanic soils compared to sands and clays. Majority of the studies on the mechanics of decomposed volcanic rocks are at large strain (*e.g.,* Okewale and Coop 2017, 2018a, 2018b; Rocchi *et al.* 2015). The knowledge about the material that is still very limited despite the usefulness of the materials in engineering construction can have serious consequences because majority of geotechnical problems are caused by these geomaterials, for example, landslides in Hong Kong and earthquake-induced disasters such as liquefactions and slope failure in Japan.

Mechanical behaviour (strength and stiffness) of soils is affected by particle breakage that occurs during loading and deformation (*e.g.,* Hardin 1985; Nanda *et al.* 2017; Okewale 2019a). For example in isotropic compression, the deformation produces primarily volume change and the particle breakage adds to the reduction in volume change. Factors such as particle size, shape and strength, particle grading, void ratio and effective stress are the determinants of the amount of particle breakage in the soil. Majority of the studies usually linked particle breakage to the strength but it can also be linked to stiffness particularly at small strain. There are very few studies relating particle breakage to small strain shear modulus for soils (*e.g.,* Nanda *et al.* 2017) and much scarce for decomposed volcanic soils.

This paper presents small strain shear modulus and breakage of uniformly graded volcanic soils, evaluating the breakage of particle during the tests and relate it to G_{max} as well as total energy input. Predicting mechanical properties especially deformation characteristics required for design is crucial at the beginning of project where data may not be available and using the relationship that includes properties (void ratio, mean effective confining stress, grading descriptors and particle shape) that can easily be measured to estimate G_{max} will be of great importance and interesting. In view of this, new model equation is developed for predicting G_{max} of volcanic soil and G_{max} of the samples is predicted using empirical equation suggested by Payan *et al.* (2016) which has been used for other geomaterials (*e.g.,* Li and Senetakis 2017) that considered the combined effects of void ratio, mean effective confining stress, grading descriptors and particle shape, and the measured G_{max} from experimental data is related to predicted G_{max} in a systematic way. Furthermore, an attempt is made to compare the new model equation with the equation suggested by Payan *et al.* (2016).

Manuscript received July 2, 2019; revised October 25, 2019; accepted November 25, 2019.
[1*] Lecturer (corresponding author), Department of Mining Engineering, Federal University of Technology Akure, Ondo State, Nigeria (e-mail: iaokewale@futa.edu.ng), University of Johannesburg, South Africa.
[2] Professor, University of Johannesburg, South Africa.

This study is very essential because weathered volcanic soils are abundant in Hong Kong and many potential hazards and geotechnical problems occur in them. Also, small strain shear modulus is important in dynamic loading studies such as earthquake engineering. Also, estimating the particle breakage provides further insight into the mechanical behaviour of the soils and the influence of breakage on G_{max}. The study is also novel in the way the new expression is developed for decomposed volcanic soil. This is also new because there has never been a systematic study on volcanic soils linking the breakage to small strain shear modulus as presented in this work. Although the original gradings of the soil used in this work is well-graded, uniformly graded samples were used because the empirical equation was developed from sands which were relatively uniform (C_u < 10) compared to the original state of the investigated soil in this study (C_u = 428). It is anticipated that this can be considered as a first step in solving a more complex problem.

This study is however different from Okewale (2019b) which investigated the effects of weathering on the stiffness characteristics and the small strain behaviour of decomposed volcanic rocks in the intact and reconstituted states thereby allowing for the effects of structure. This was achieved by conducting many bender elements testing on volcanic soils. This technique involves converting shear wave velocity v_s to G_{max}.

2. SOILS TESTED

The soils tested were obtained from coarse-grained completely decomposed volcanic rocks. The parent rock is locally called tuff. Decomposed volcanic soils are formed from physical and chemical processes of weathering of parent rock. The soil comprises quartz, feldspar and clay minerals. The weak minerals particularly feldspar have decomposed into clay minerals (kaolinites) and part of the feldspar and quartz are present in the resulting soils. The decomposed volcanics is completely different from the samples tested by Okewale and Coop (2017, 2018a, 2018b) and Okewale (2019a, 2019b, 2019c, 2020). The sample was collected as block and was retrieved at 1.5 ~ 2.5 m. The sample belonged to extremely weak to weak completely decomposed volcanic rocks (ewwCDV) of Mt Davis formation, which is coarse grained. The map of sample location is given in Fig. 1.

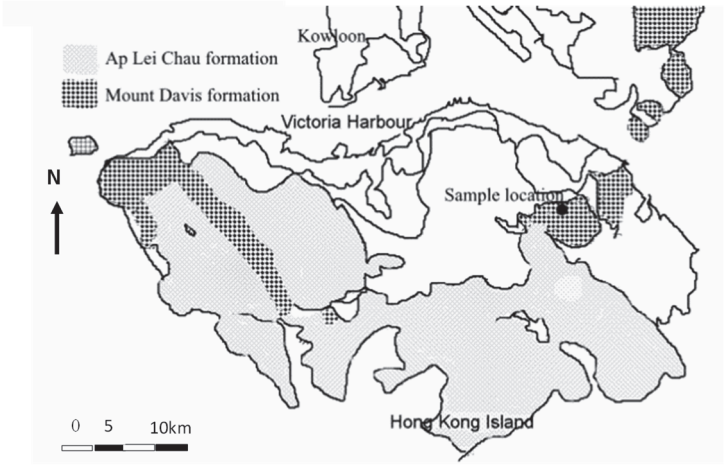

Fig. 1 Map of sample location in Hong Kong

The particle size distribution of original soil was obtained from wet sieving and sedimentation technique as presented in Fig. 2. The soil is well-graded with 11% clay, 17% silt, and 72% sand fractions. The mean particle size is 0.3 mm and the coefficient of uniformity is 428. The liquid limit was found to be 34.6% and it was non-plastic. The liquid limit was determined according to ASTM D4318. The Atterberg limit test was carried out on the fine fraction of the investigated soil to show the index properties of the soil in terms of plasticity. The soils tested in this study are artificially separated and classified based on their particle sizes namely: silt soil (Si) which comprises silt and clay fractions, fine sand soil (FS), fine/medium sand soil (FMS), medium sand soil (MS) and coarse sand soil (CS). Samples are separated into different sizes because reconstituted samples are common in the construction of engineering structures. Five volcanic soils which are uniformly graded and composed of different particle shapes were used. The particle size distributions of the soils obtained using dry sieving is presented in Fig. 3.

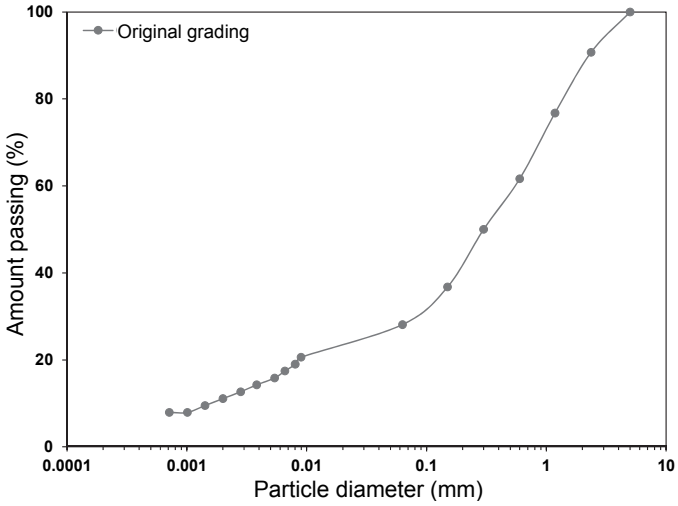

Fig. 2 Particle size distributions for the original soil

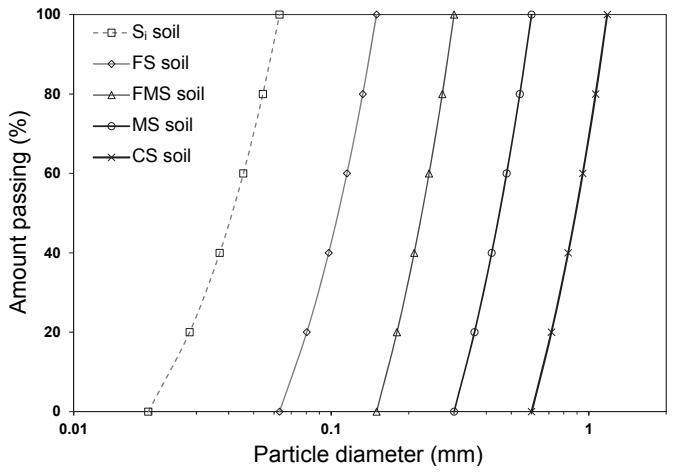

Fig. 3 Particle size distributions for the soil; Si silt, FS fine sand, FMS fine/medium sand, MS medium sand, CS coarse sand

The details of the characteristics of the soils are given in Table 1. As expected, the median particle size (d_{50}) of the soils increases with soils from silt to coarse sand soil. Also, the coefficient of uniformity (C_u) shows that the soils are not well-graded due to very low values which is reducing with increasing particle sizes. The particle shape descriptors namely, sphericity S which denotes the overall configuration of the particle shape, roundness R which is the descriptions of the corners of the particles and regularity ρ that combines S and R are also given in the Table 1 but will be discussed in the results and discussions section. The details of the tests are given in Table 2. The test descriptions indicate the soil code, followed by the test number and then the state of the test.

Table 1 Details of basic characteristics of the soils

CDV soils type	Silt (Si)	Fine sand (FS)	Fine/medium sand (FMS)	Medium sand (MS)	Coarse sand (CS)
d_{50} (mm)	0.03	0.10	0.23	0.45	0.89
C_u	1.75	1.64	1.50	1.45	1.39
S	0.60	0.62	0.61	0.65	0.66
R	0.38	0.41	0.40	0.42	0.42
ρ	0.49	0.52	0.51	0.54	0.54

Note: d_{50} mean particle size, C_u coefficient of uniformity, S sphericity, R roundness, ρ regularity

3. METHODOLOGY

The samples were prepared by using specially designed two part split moulds. The split moulds were of 50 and 60 mm diameters and 100 and 120 mm heights given samples of height to diameter ratio of 2:1. The samples were prepared directly on the triaxial apparatus at different initial void ratios. The membrane and mould were put in place. They were then supported by vacuum to keep the membrane very firm. The samples were prepared by carefully pouring the dry material from a small height into the mould in five or six layers. The samples were then compacted lightly after each layer using a light weight plastic rod with light weight steel round edge. However, care was taken so that the particles do not break during sample preparations. The samples were prepared to have different initial void ratios. Relative density is defined as the ratio of the difference between maximum void ratio (e_{max}, loosest state) and in situ (field) void ratio (e) to the difference between maximum (e_{max}) and minimum void ratios (e_{min}, densest state). This was not calculated for this study and it will be difficult to suggest corresponding relative density to initial void ratio. Based on literature, it is believed that soil with the same relative density although with different void ratios will behave in similar way under loading and based on this, relative density is preferred to void ratio. However void ratio is used in this study because it is considered as a fundamental property of geomaterials because it is combined with stress to describe the behaviour of geomaterials.

Two Imperial College (IC) stress path triaxial apparatuses were used. The IC cells have cell capacity of 800 kPa and equipped with 50 mm and 60 mm diameter platens. They were also equipped with local instrumentations and bender elements (Pennington *et al.* 1997; Clayton *et al.* 2004) for the determination of small strain shear moduli of the soils. The bender elements (BE) are powerful transducer used to determine shear wave velocity which then gives small strain shear modulus. After sample preparation and before applying confining pressure, a suction of about 10 kPa was applied. The vacuum was then removed during the first loading stage. The samples were loaded in isotropic condition in a continuous way and the measurements of bender element were taken in different stages.

The tests were conducted at mean effective confining pressures of 50, 100, 200, 400, and 680 kPa. The BE was excited with a single shot sine wave with wide range of frequencies (10 ~ 13 kHz). Both input and output frequencies were measured and recorded by an oscilloscope. The shear wave velocity of the samples was calculated using first arrival time method (Fig. 4). The first thing is identifying the arrival time (t_a) and then the velocity (v_s) of the travelling wave can be determined using distance between the tips of the bender elements. Figure 4 shows the determination of arrival time for different frequencies. Consequently, small strain shear modulus (G_{max}) is obtained using the equation;

$$G_{max} = \rho_b \, v_s^2 \tag{1}$$

where ρ_b is the bulk density of the soil.

The void ratios (e) were obtained by careful measurements of initial dimensions (height and diameter) and weights while the sample was supported by suction immediately after the sample preparation.

In order to account for the effect of particle shape, it is very important to describe it in a numerical way. The empirical chart (Fig. 5) proposed by Krumbein and Sloss (1963) was used to determine the values for the different particle shapes. In Fig. 5, three descriptors namely, sphericity S which is the ratio between the radius of the inscribed sphere in the particle to the radius of the smallest circumscribed sphere to the particle, roundness R the ratio of the average radius of curvature of the surface feature to the radius of the largest sphere inscribed in the particle and regularity (ρ), which is the arithmetic mean of S and R (Cho *et al.* 2006) can be used. However, the repeatability of the shape for different soils was determined by selecting twenty particles randomly and these particles were observed under an optical microscope. The mean value of the descriptors for each soil are given in Table 1 and the values are similar, indicating that the shapes are fairly similar. Close values of the parameters indicate that the shapes of the volcanic soils of different particle sizes are fairly similar. This is similar to what has been found by Okewale (2019a, 2019c) studies on similar volcanic soils.

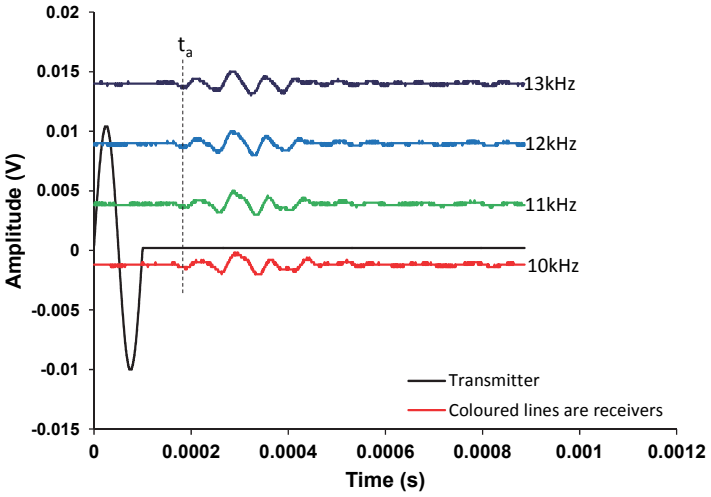

Fig. 4 Typical bender element plots to determine arrival time

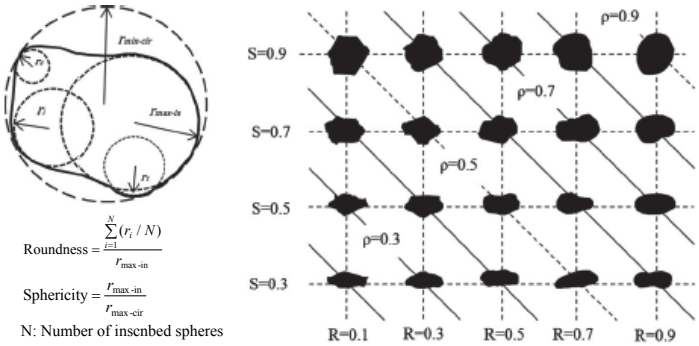

Fig. 5 Particle shape characterisation chart modified from Krumbein and Sloss (1963) (after Payan *et al.* 2016)

4. RESULTS AND DISCUSSIONS

4.1 Variation of Small Strain Shear Modulus with Confining Pressure and Void Ratio

The BE tests for soils are presented in Fig. 6. The figure is however shown for each soil separately for clarity. The empirical power law equation that relates small strain shear modulus (G_{max}) with mean confining pressures (p') (Eq. (2)) is used to express the modulus of the soils.

$$G_{max} = A \times f(e) \times \left(\frac{p'}{p_a}\right)^n \quad (2)$$

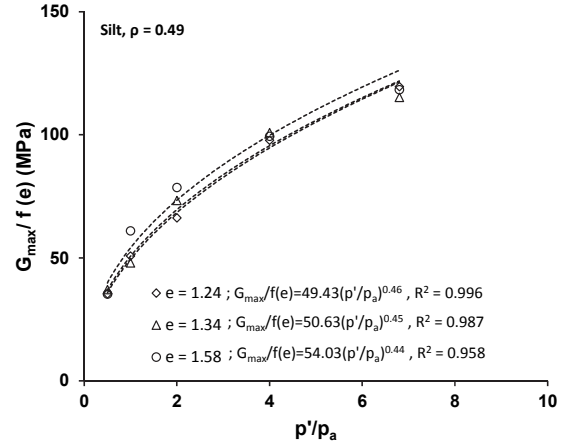

(a) Silt

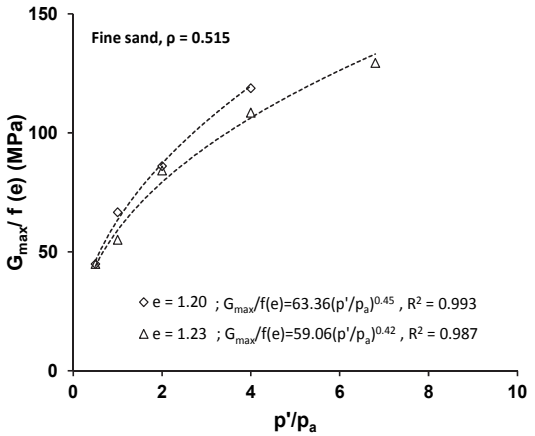

(b) Fine sand

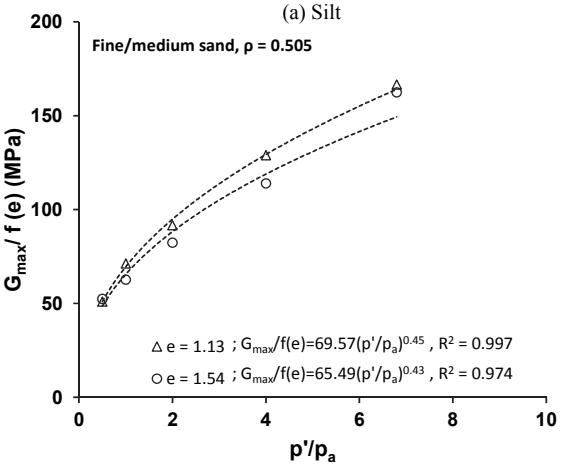

(c) Fine/medium sand

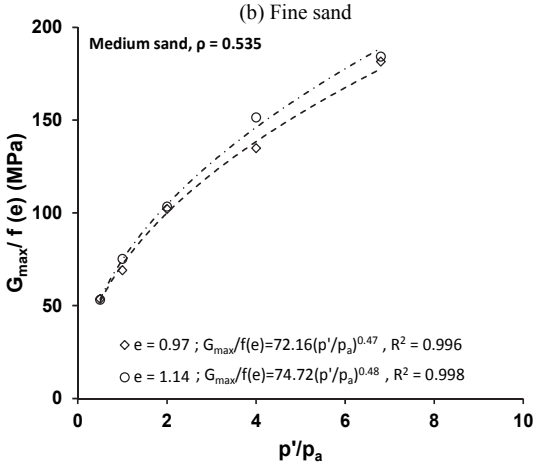

(d) Medium sand

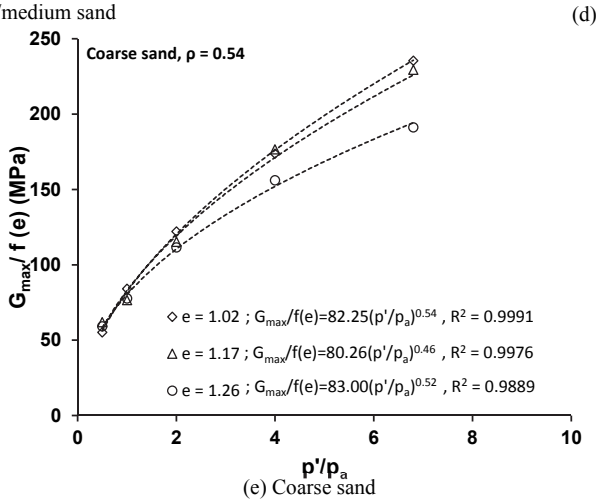

(e) Coarse sand

Fig. 6 Variation of normalized small strain shear modulus with normalised confining pressure for soils with different void ratios

where p_a is reference atmospheric pressure (p_a = 100 kPa), $f(e)$ is void ratio function and A and n are model parameters to be determined from experimental data. This power law is similar to the one used for decomposed volcanics studied by Okewale (2019b). Several void ratio functions were considered but the one proposed by Jamiolkowski *et al.* (1995) ($f(e) = e^{-1.3}$) was used because it has been used for weathered igneous rocks (*e.g.,* Rocchi and Coop 2015). The variations of normalised small strain shear modulus ($G_{max}/f(e)$) with normalised confining pressure (p'/p_a) with different void ratios are presented. The average regularity (ρ), the relationships between $G_{max}/f(e)$ and p'/p_a for different void ratios as well as coefficient of determination (r^2 value) of the regression equations are also given in the plot.

Small strain shear modulus increases with mean effective stress for the soils similar to what has been found for other geomaterials. Although the material parameter A seems increasing with initial void ratio for some soil but there is no particular trend after normalisation. Parameter A varies for different soils and it increases from silt to coarse sand soil. Parameter n are relatively close for different soils indicating fairly similar particle shape. The G_{max} increases from silt to coarse sand soil and this can be attributed to increase in the density of the sample.

Figure 7 presents the behaviour of soils in isotropic compression. The results are shown in e-log p' plane. The result is shown for one test in each soil for clarity. The compression curves are similar for the soils. Apart from little scatter, soils with smaller particle size plot above those with larger particle size.

Figure 8 shows the variation of G_{max} with void ratio for the soils. The relationship between G_{max} and void ratio is shown for only coarse sand soil for clarity. The small strain shear modulus reduces with void ratio as expected.

4.2 Variation of Particle Breakage with G_{max}

In order to determine the amount of particle breakage, the relative breakage B_r proposed by Hardin (1985) was used and it is defined as the ratio of total breakage B_t to the breakage potential B_p ($B_r = B_t/B_p$). Figure 9 shows the determination of B_r which is given as the ratio of the area between the grading curves before and after the test considering only the part above 0.074 mm (B_t = area BCDB) to the area between the initial grading curve and a cut-off at 0.074 mm (B_p = BCAB). Since B_r is limited to particle size greater than 0.074 mm, the B_r is not estimated for silty soil.

Figure 10 presents changes in particle size distribution curves for the soils as a result of particle breakage. This indicates that particle breakage occurs in the samples of fine sand, fine/medium sand, medium sand and coarse sand. The particle breakage which is indicated by the offset between initial grading and the grading after the test has been isotropically compressed to 680 kPa is increasing with soil fraction (Figs. 10(a) to 10(d)). The particle breakage increases from fine sand to coarse sand. Figure 11 presents the variation of particle breakage with small strain shear modulus of the soils. The breakage increases with $G_{max}/f(e)$ and the increase in $G_{max}/f(e)$ can be attributed to greater number of particles to particle contacts resulting from particle breakage. This behaviour is similar to what has been found for other geomaterials (*e.g.,* Nanda *et al.* 2017).

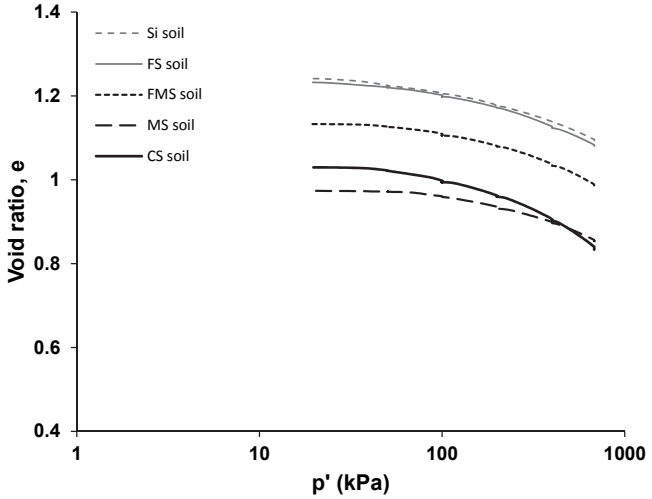

Fig. 7 Behaviour of soil in e: log p' plane

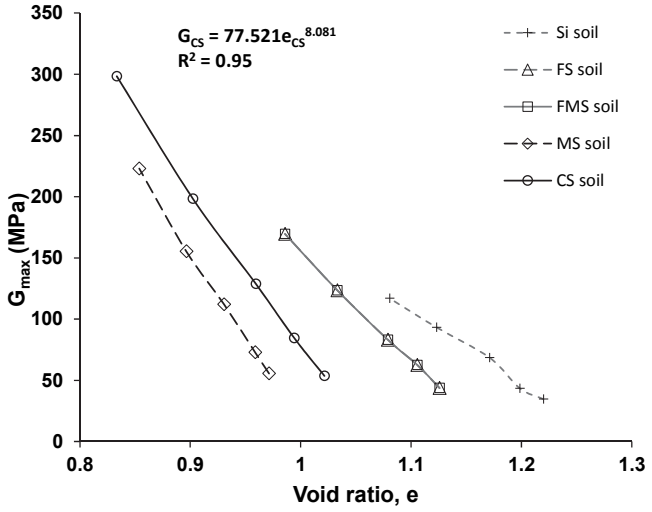

Fig. 8 Variation of G_{max} with void ratio

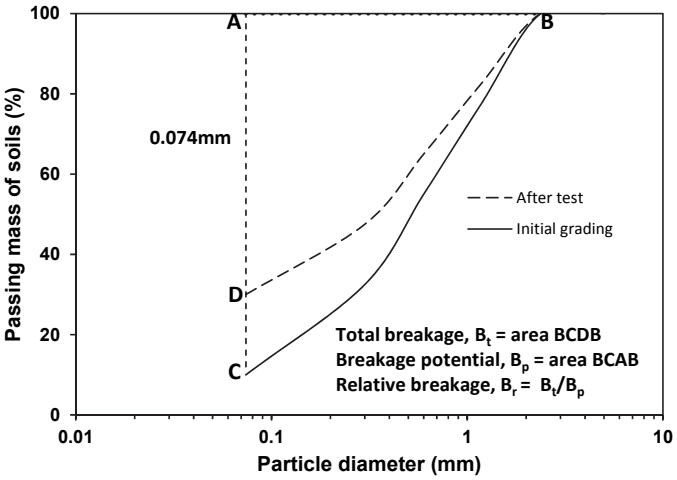

Fig. 9 Determination of relative breakage (B_r) using method proposed by Hardin (1985)

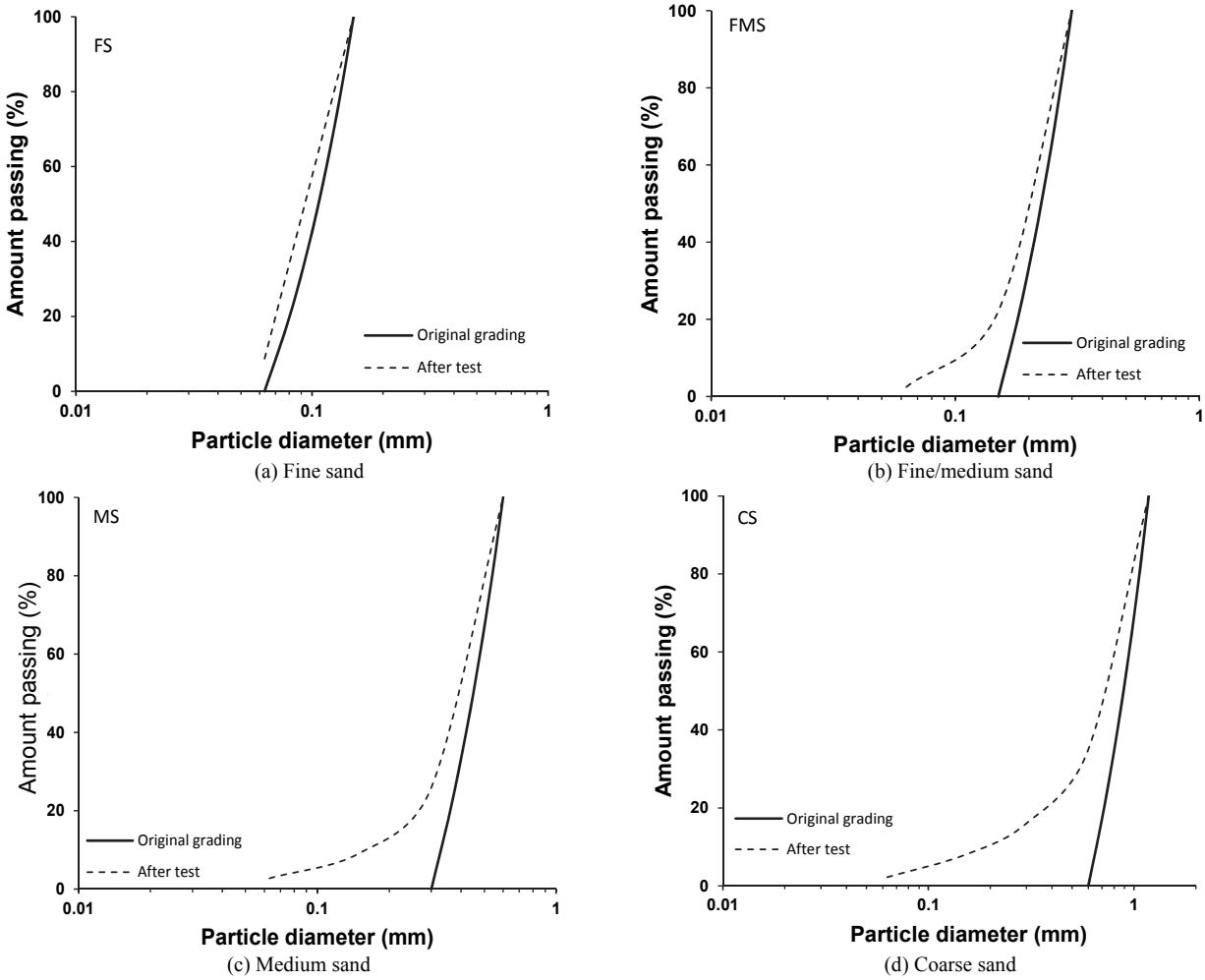

(a) Fine sand (b) Fine/medium sand

(c) Medium sand (d) Coarse sand

Fig. 10 Changes in particle size distribution curves resulting from particle breakage for the soils

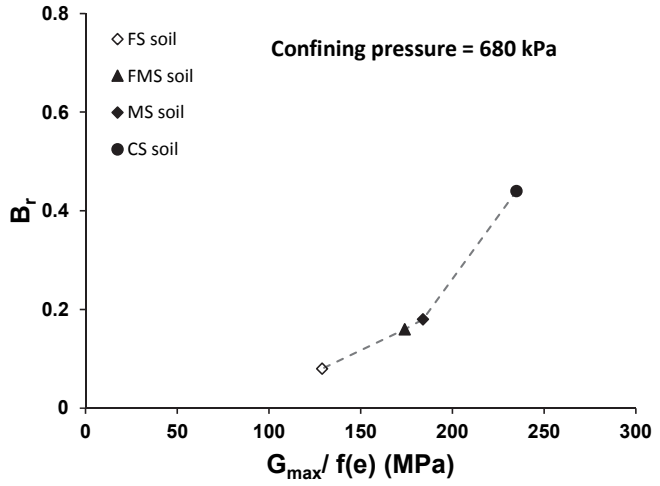

Fig. 11 Variation of particle breakage with small strain shear modulus

It has been suggested that particle breakage should be related to total energy input (E_T) rather than mean effective stress because breakage depends primarily on the amount of energy absorbed by the soil sample (Lade *et al.* 1996; Nanda *et al.* 2017). Lade *et al.* (1996) stated that the total amount of energy input per unit volume of sample during triaxial test is the sum of energy input during isotropic compression and shearing.

$$E_T = E_C + E_S \tag{3}$$

where E_T is total energy input per unit volume of the sample, E_C is energy input during isotropic compression and E_S is the energy input during shearing. The equation can further be expressed as

$$E_T = \sum_{SOT}^{BOS} \sigma_c \, \varepsilon_v + \left[\sum_{BOS}^{EOS} (\sigma_1 - \sigma_3) \, \varepsilon_a + \sum_{BOS}^{EOS} \sigma_c \, \varepsilon_v \right] \tag{4}$$

where σ_c is average confining pressure, ε_v is volumetric strain increment, $\sigma_1 \sim \sigma_3$ is average stress difference, ε_a is axial strain increment, SOT is start of test, BOS is beginning of shearing and EOS is end of shearing. Since the test involved in this study is isotropic compression only, the equation reduces to:

$$E_T = \sum_{SOT}^{EOC} \sigma_c \, \varepsilon_v \tag{5}$$

where EOC is the end of compression. The merit of this approach is that the particle breakage is linked to both stress and strain.

Figure 12 presents the variation of particle breakage relative to mean effective stress and total energy input. Soils were isotopically compressed to the same mean effective stress so that the effect of mean stress on the breakage will be the same (Fig. 12(a)). Figure 12(b) shows the relationship between breakage and total

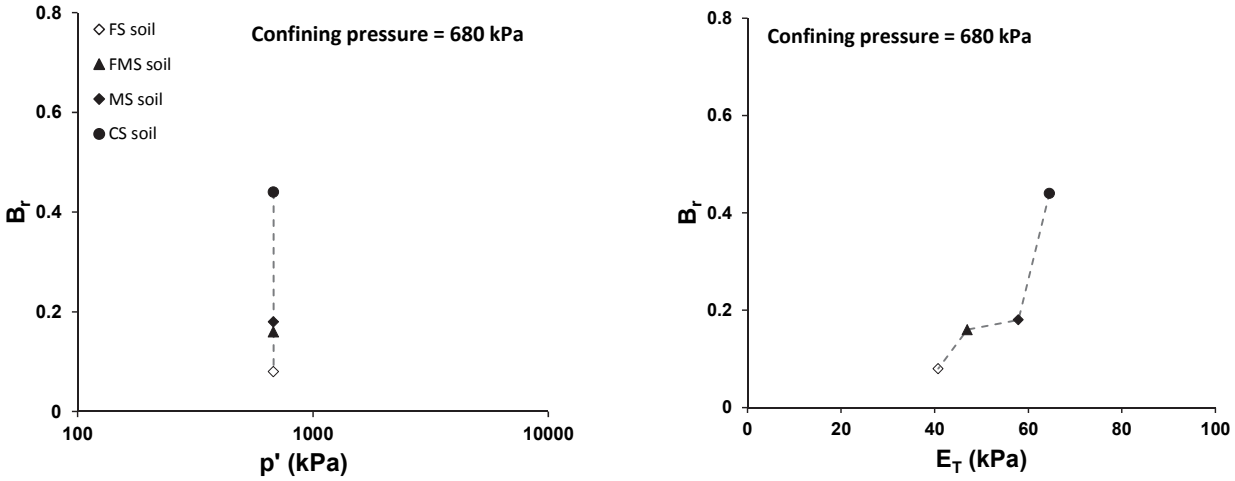

(a) Mean effective stress (b) Total energy input

Fig. 12 Variation of particle breakage with mean effective stress and total energy input

energy input estimated using Eq. (5). A clear trend of increase in particle breakage with the total energy can be seen, similar to what has been found by other studies. This shows that total energy approach is very useful in describing particle breakage in decomposed volcanic soils because of the strain inclusion.

4.3 Development of G_{max} Expression from Experimental Data

A new expression is developed from experimental data by employing power type equation similar to Eq. (2) that incorporates effect of particle shape and void ratio. The equation in its general form can be written as;

$$G_{\max} = A(C_u, d_{50}, \text{shape}) \times e^{x(C_u, d_{50}, \text{shape})} \times \left(\frac{p'}{p_a}\right)^{n(C_u, d_{50}, \text{shape})} \quad (6)$$

where the model parameters A, x and n are functions of grading descriptors and particle shape. The coefficients of best fit to the data (Fig. 5) were used to establish the relationships between A and n and the grading descriptors for the volcanic soil. The details of the parameters are given in Table 2. Figures 13(a) and 13(b) show the variation of parameters A and n with mean particle size d_{50} respectively. The relationships between the parameters and mean particle size is also given in the figure. As can be seen from the figure, parameter A is increasing with mean particle sizes and n values seem increasing but insignificantly with d_{50}.

It has been found that mean particle size (d_{50}) has a negligible influence on parameters A and n (Senetakis *et al.* 2012; Saxena and Reddy, 1989) and d_{50} and coefficient of uniformity (C_u) have little influence on x (Senetakis *et al.* 2012). Also it has been found that particle shape does not influence x. If the effects grading descriptors and particle shape on parameters A and n are separated, Equation 6 can be reduced to;

$$G_{\max} = A_1(C_u) \times A_2(\text{shape}) \times e^{x(C_u)} \times \left(\frac{p'}{p_a}\right)^{n_1(C_u) \times n_2(\text{shape})} \quad (7)$$

The effects of coefficient of uniformity and particle shape on model parameters are determined from experimental data.

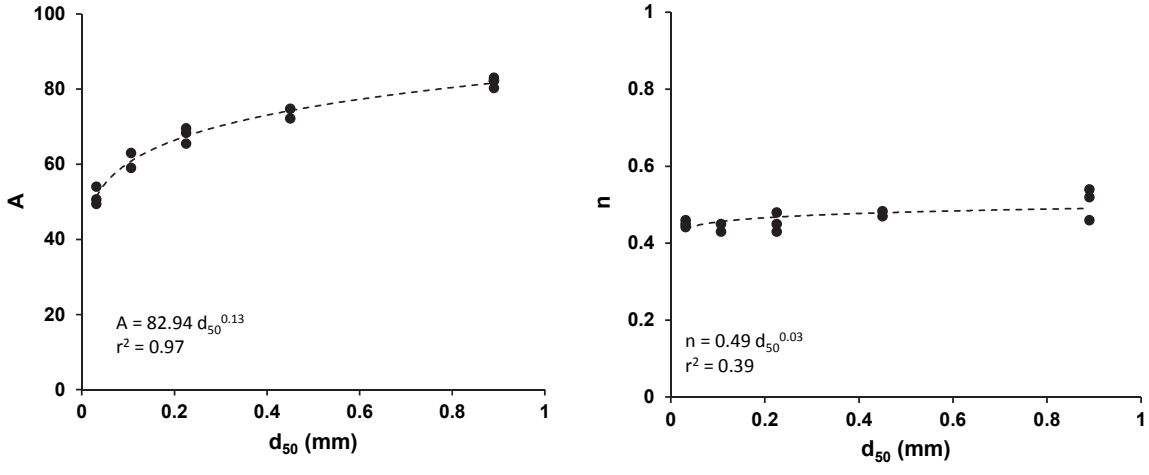

(a) A (b) n

Fig. 13 Variation of parameters with mean particle size d_{50}

Table 2 Details of bender element tests

Sample	Test	e_0	p_c' (kPa)	A (MPa)	n
Silt	S01D	1.58	680	54.0	0.44
	S02D	1.34	680	50.6	0.45
	S03D	1.24	680	49.4	0.46
Fine sand	FS01D	1.23	680	59.1	0.43
	FS02D	1.20	400	63.4	0.45
Fine/medium sand	FMS01D	1.54	680	65.5	0.43
	FMS03D	1.13	680	69.6	0.45
Medium sand	MS01D	1.14	680	74.7	0.48
	MS02D	0.97	680	72.2	0.47
Coarse sand	CS01D	1.26	680	83.0	0.52
	CS02D	1.17	680	80.3	0.46
	CS03D	1.02	680	82.3	0.54

Note: e_0 initial void ratio, A and n stiffness constants, p_c' mean effective stress at the end of test

The variation of parameters A_1 and n_1 with coefficient of uniformity is presented in Figs. 14(a) and 14(b). The A_1 values reduce with C_u similar to what has been found for sands studied by Payan *et al.* (2016) and n_1 does not show significant change with C_u. Applying a power best-fit trend, the following relationships are found for the variation of A_1 and n_1;

$$A_1 = 151.42 \times C_u^{-1.918} \tag{8}$$

$$n_1 = 0.56 \times C_u^{-0.46} \tag{9}$$

In order to determine effects of particle shape descriptor (ρ) on the parameters A_2 and n_2, the A and n values obtained from experimental data are normalized with respect to the expressions of A_1 and n_1 presented in Eqs. (8) and (9) respectively. This allows the effects of ρ on A_2 and n_2 to be isolated as presented in Figs. 15(a) and 15(b). The A_2 and n_2 can be given as;

$$A_2 = \frac{A}{151.42 \times C_u^{-1.918}} \tag{10}$$

$$n_2 = \frac{n}{0.56 \times C_u^{-0.46}} \tag{11}$$

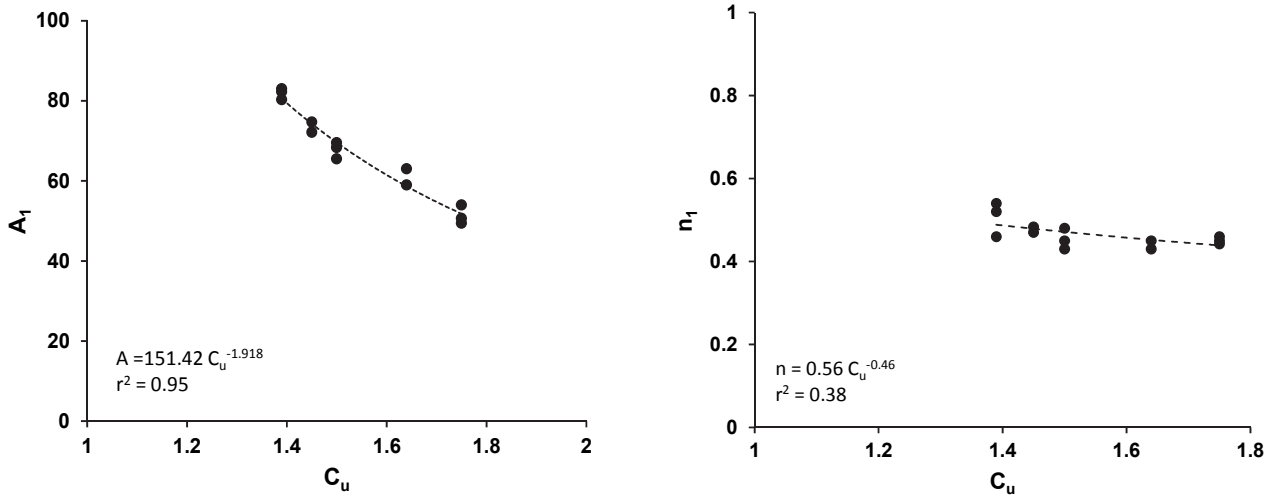

(a) A_1 (b) n_1

Fig. 14 Variation of parameters with coefficient of uniformity C_u

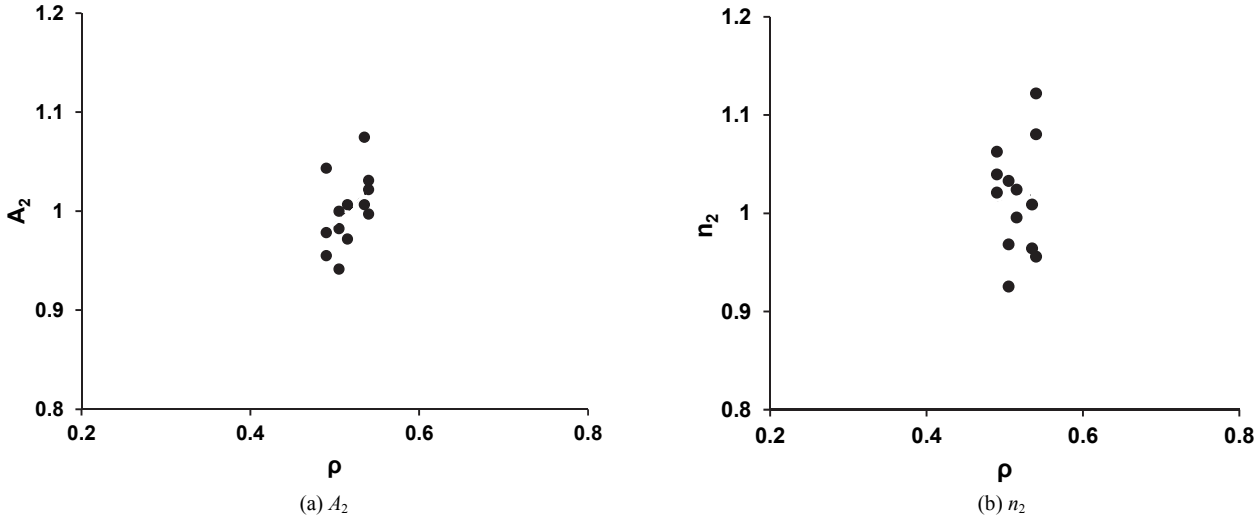

(a) A_2 (b) n_2

Fig. 15 Variation of parameters with regularity ρ

The relationships between the parameters and ρ yield poor correlation because the particle shape of the soils tested are fairly similar. To establish the effects of C_u on void ratio power x, it requires conducting tests on soil at constant particle shape and constant confining pressure according to Payan *et al.* (2016). The test conducted in this work is different from this. However, attempt was made and the relationship for coarse sand is given in Fig. 8 but was not used. For this study, a constant value of $x = -1.3$ is assumed because it has been used for similar soil and very close to the value ($x = -1.29$) obtained by Payan *et al.* (2016) and also consistent with other studies (*e.g.,* Jamiolkowski *et al.* 1995; Senetakis *et al.* 2012). This leads to;

$$f(e) = e^{-1.3} \tag{12}$$

Combining the best-fit Eqs. (8) and (9) and Figs. 15(a) and 15(b) derived for model parameters, G_{max} expression that considers the effects of void ratio, particle size distribution, particle shape and confining pressure can be given as;

$$G_{\max} = (203 C_u^{-1.92}\, \rho^{0.45}) \times e^{-1.3} \times \left(\frac{p'}{p_a}\right)^{(C_u^{-0.46})\times(0.11\rho+0.51)} \tag{13}$$

The model expression (Eq. (13)) was used to predict G_{max} of different soils used in this work and comparison is made with measured G_{max} as presented in Fig. 16. The new equation is able to predict the soils accurately with very significant regression statistics ($r^2 = 0.99$ and p-value = 6.83E–54).

4.4 Prediction of G_{max} of Volcanic Soil Using Model Expression of Payan *et al.* (2016)

Attempts are made to predict small strain shear modulus of decomposed volcanic soils using empirical equation proposed for the sand by Payan *et al.* (2016) and used by Li and Senetakis (2017);

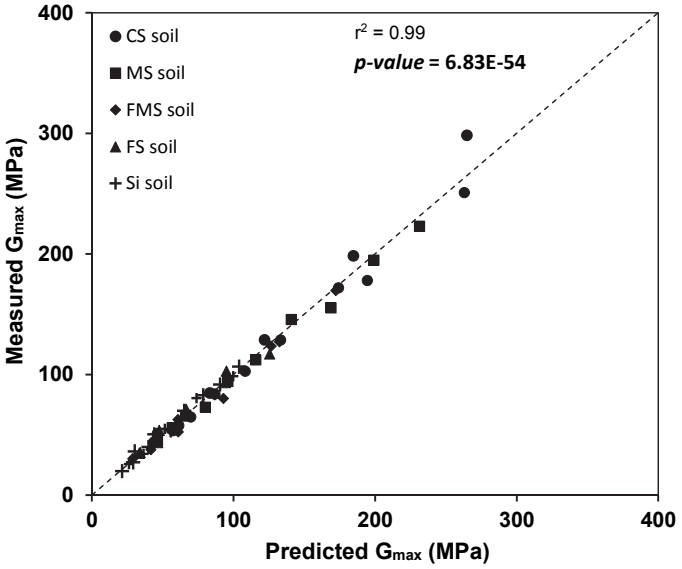

Fig. 16 Variation of measured G_{max} with predicted G_{max} using developed model equation

$$G_{\max} = (84\, C_u^{-0.14}\, \rho^{0.68}) \times e^{-1.29} \times \left(\frac{p'}{p_a}\right)^{(C_u^{0.12})(-0.23\rho+0.59)} \tag{14}$$

Equation (14) incorporates the particle size distribution, particle shape, void ratio and confining pressure. This equation is used in this work to predict the G_{max} and the results are compared with measured G_{max} as shown in Fig. 17. This expression is used because it is the first formula proposed in the literature for the elastic stiffness which incorporates both grain size characteristics and particle shape into a single expression. The equation was developed for sand and it should be able to be applied to volcanic soils that comprise grains from weathered rocks. As stated earlier, predicting G_{max} is necessary at preliminary design stage where stiffness data may not be available for geotechnical design. Therefore, the equation can be used as a guide to estimate G_{max} of the soil.

As can be seen in Fig. 17(a), the data points plot on the line of perfect prediction. The expression predicts the modulus of silt soil accurately and satisfactorily, similar to what has been found other materials (*e.g.,* Li and Senetakis 2017). The broken lines in the plots indicate the perfect prediction of moduli which means the ratio of measured to predicted G_{max} is 1. The modulus of fine sand is fairly predicted by the equation (Fig. 17(b)) due to little scatterness of the data around the line of perfect prediction. In Figs. 17(c) and 17(d), the moduli of fine/medium sand and medium sand are poorly predicted. However, the coarse sand modulus is very poorly predicted (Fig. 17(e)). It can be seen that the ease of predicting the moduli of soils is reducing as the coarseness of the soil is increasing.

It has been suggested that other methods such as plotting the normalised modulus again state parameter (Been and Jefferies, 1985) can be used for prediction. State parameter can only be defined from critical state data and only few critical state data from monotonic triaxial tests (Okewale 2017) available are for original sample and cannot be used for this work.

Attempt is also made to compare the new model equation developed in this study (Eq. 13) to the equation proposed by Payan *et al.* (2016) (Eq. 14). Figure 18 presents the comparison between Eqs. (13) and (14) for different volcanic soils studied. The regression statistics and line of perfect prediction are also given in each plot. The regression statistics were carried out for each soil and the coefficient of determination r^2 and p-value are used as statistical parameters. The r^2 is the quantitative strength of the relationship between the predicted G_{max} using Eq. (13) and predicted G_{max} using Eq. (14) and p-value shows the probability of true relationship between the two predicted G_{max}. The relationships are perfect for both silt and fine sand soils with very strong correlation statistics and convergence of data around lines of perfect prediction (Figs. 18(a) and 18(b)). There are strong relationships between the two model equations but the data are diverging for fine/medium sand and medium sand soils (Figs. 18(c) and 18(d). The regression statistics for coarse sand soil are not too strong and the data are diverging from line of perfect prediction (Fig. 18(e)). This shows that the equation proposed by Payan *et al.* (2016) can only predict accurately the silt and fine sand soils of decomposed volcanics.

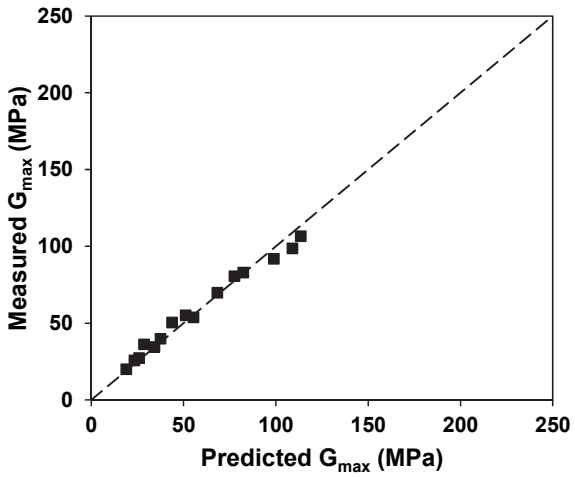

(a) Si soil

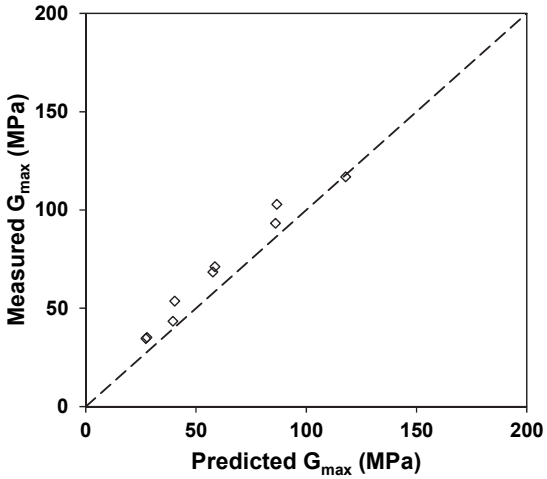

(b) FS soil

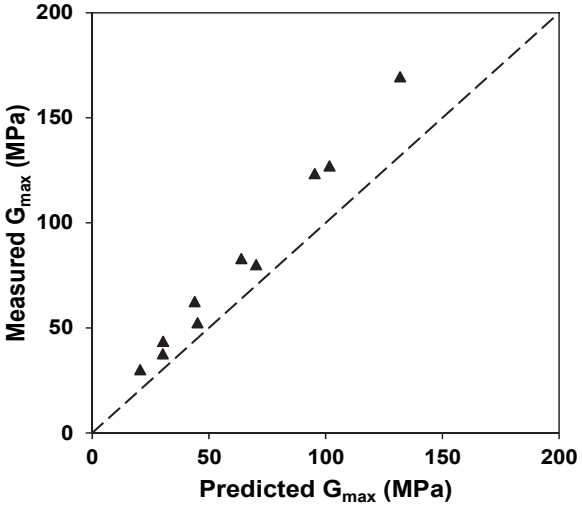

(c) FMS soil

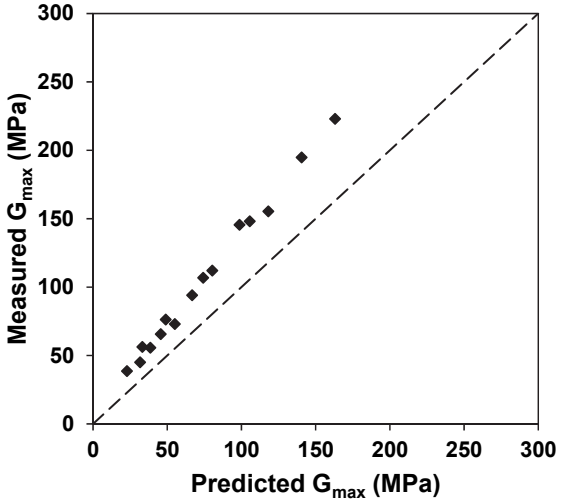

(d) MS soil

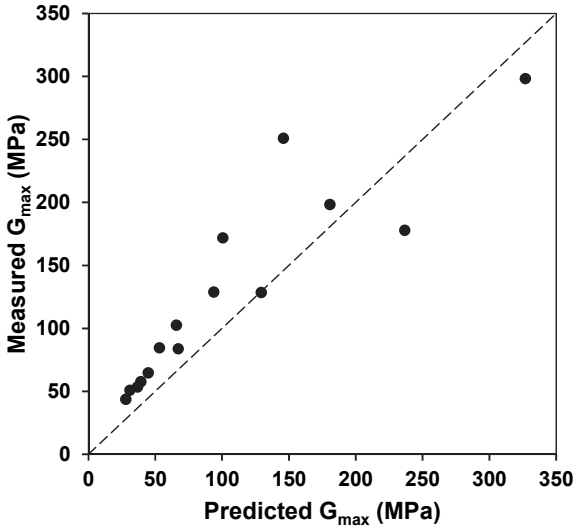

(e) CS soil

Fig. 17 Measured against predicted elastic shear modulus for the soils using Payan *et al.* (2016) equation

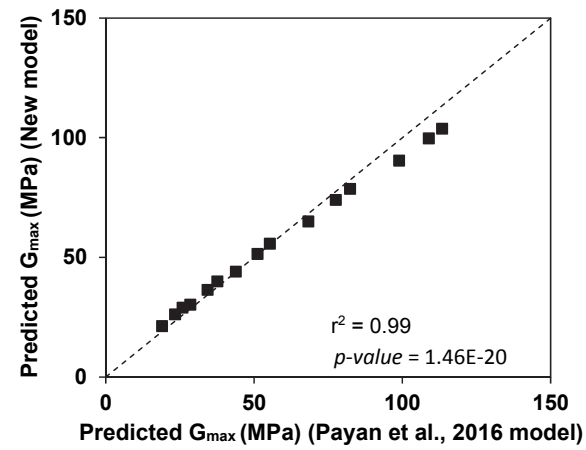

(a) Si soil

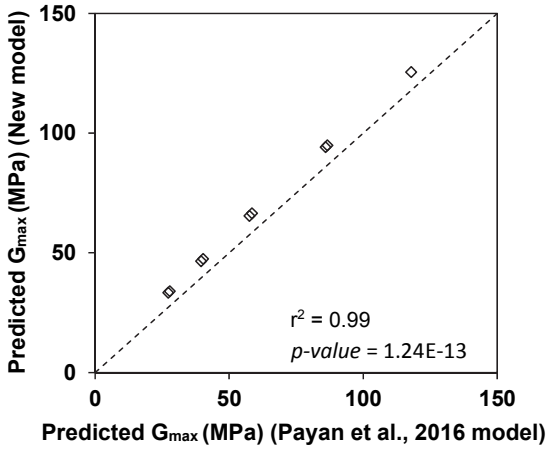

(b) FS soil

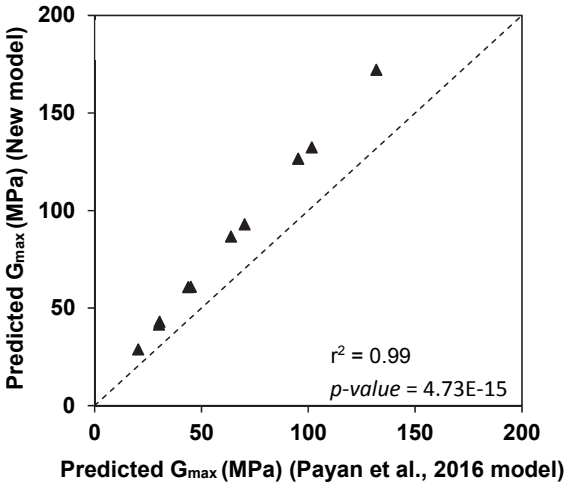

(c) FMS soil

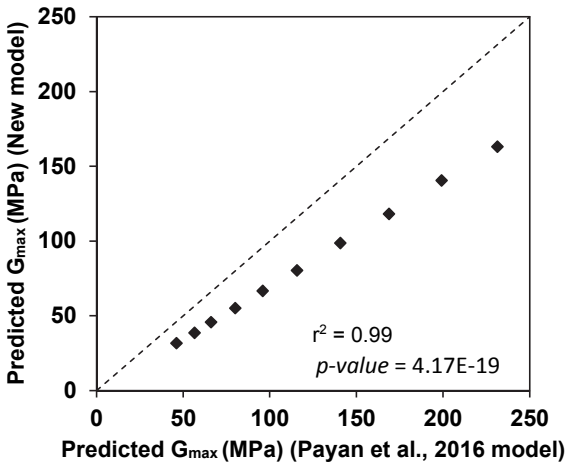

(d) MS soil

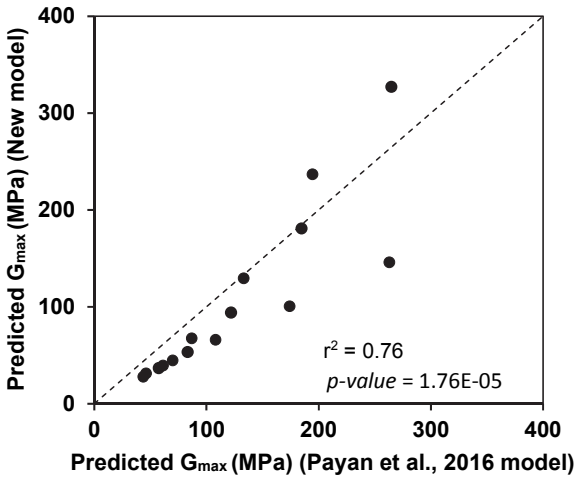

(e) CS soil

Fig. 18 Comparison of the new model equation and Payan *et al.* (2016) equation

In order to quantify the degree of predictability of the moduli of the soils, preliminary attempts are made by calculating the deviation of the data from the perfect line of prediction in percentages and regression statistics and the results are presented in Fig. 19. The correlation statistics are given in each plot. Generally, there is a very strong correlation between measured and predicted G_{max} but the coarse sand soil has the least value. The value of deviation seems increasing as the coarseness of soil is increasing (Figs. 19(b) to 19(e)). This indicates that the ease of predicting G_{max} is reducing with increasing particle size of the soils.

In order to estimate the likely particle sizes at which the G_{max} may not be perfectly predicted, particle breakage and deviation from accurate prediction are related to mean particle size as presented in Fig. 20. In the figure, vertical broken line indicates the maximum particle size at which soil can be perfectly predicted and horizontal broken line shows the corresponding deviation. The value of particle size at which the G_{max} of volcanic soils can be predicted accurately is assumed to be particle size less than 0.10 mm where the deviation is around 20% based on the suggestion of study of Li and Senetakis (2017), although using different parameter (normalised modulus against state parameter).

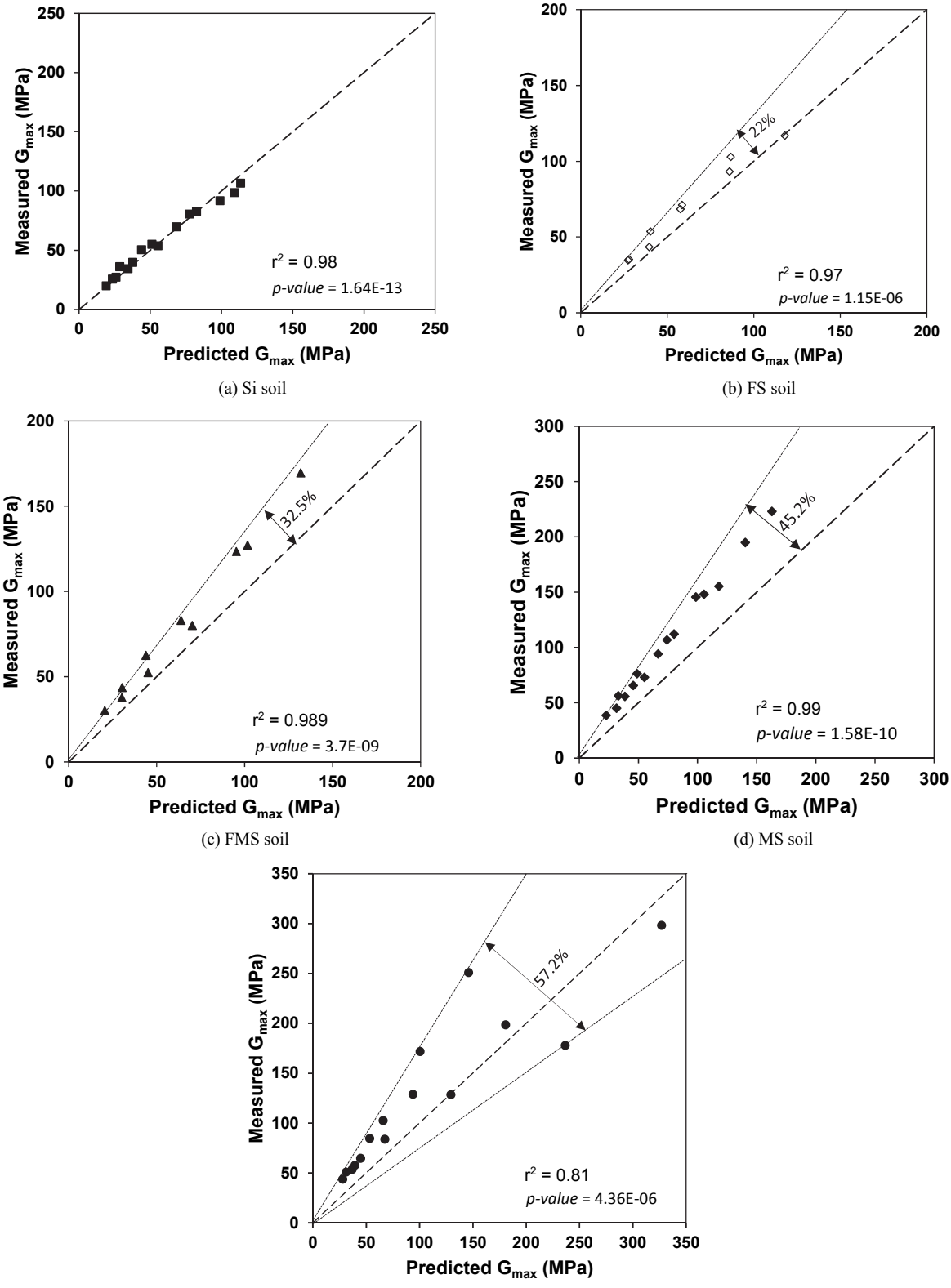

(a) Si soil

(b) FS soil

(c) FMS soil

(d) MS soil

(e) CS soil

Fig. 19 Deviation of measured against predicted elastic shear modulus for the soils

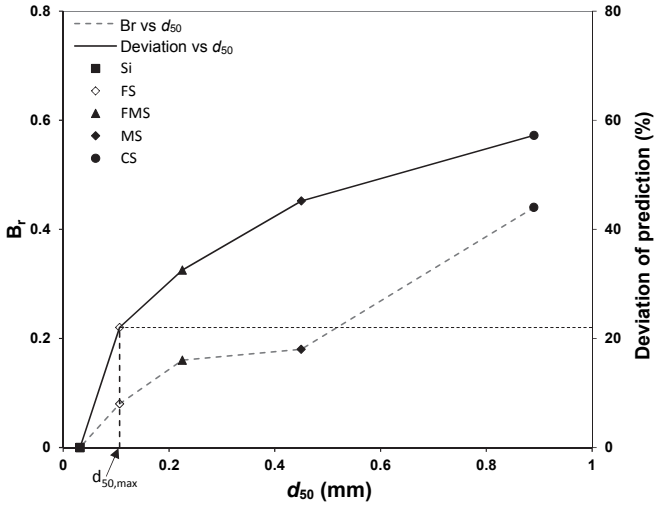

Fig. 20 Variation of particle breakage and deviation of prediction with mean particle size

5. CONCLUSIONS

Small strain shear modulus, G_{max}, and breakage of uniformly graded volcanic soils have been studied in detail. This was achieved by conducting bender element tests, estimating the particle breakage, develop a new model equation that incorporates the effects of void ratio, confining pressure, grain size distribution (coefficient of uniformity) and particle shape (regularity) and using an empirical expression proposed by Payan *et al.* (2016) to predict the small strain shear modulus of volcanic soils. Also, the effects of particle breakage on the measured G_{max} and predicted G_{max} using Payan *et al.* (2016) were studied in details.

Based on the experimental data, the small strain shear modulus increases with mean effective stress. The elastic parameter A increases with mean particle sizes and reduces with coefficient of uniformity while parameter n remains relatively unchanged with both mean particle size and coefficient of uniformity. The effect of relative density on G_{max} is not considered because void ratio was used owing to its importance in combining with stresses to describe the behaviour of soil. The particles of decomposed volcanic soils are weaker and crushable. The particle breakage increases with G_{max} and total energy input absorbed by the soils. The particle breakage is a function of strain accumulation during isotropic loading**.** The new model equation developed is used to predict G_{max} of different volcanic soils used in this study and it predicts the G_{max} of different soils accurately.

The empirical equation proposed by Payan *et al.* (2016) for sand predicts accurately the modulus of silt soil and fairly accurate for the modulus of fine sand. The equation cannot satisfactorily predict the moduli of fine/medium sand, medium sand and coarse sand. The current void ratio at a given confining pressure was used for the estimation of G_{max}. The ease of predicting moduli of volcanic soils reduces with larger fraction. The higher the coarse fraction, the higher the particle breakage and the more difficult it is to accurately predict the modulus of volcanic soil.

ACKNOWLEDGEMENTS

The author would like to thanks Civil Engineering and Development Department (CEDD) of HKSAR for the assistance in getting the samples used in this research and Mr. Thomas Tsang for making the apparatus available. The author thanks the anonymous reviewers for the valuable comments and suggestions which has really helped to improve the paper.

FUNDING

This work was fully supported by a grant from the Research Grant Council (RGC) of Hong Kong Special Administrative region (HKSAR), China (T22-603/15N).

DATA AVAILABILITY

The data and/or computer codes used/generated in this study are available from the corresponding author on reasonable request.

NOTATIONS

A	Elastic parameter obtained from experimental data
B_p	Breakage potential
B_r	Relative breakage
B_t	Total breakage
C_u	Coefficient of uniformity
d_{50}	Mean particle size (mm)
$d_{50,max}$	Maximum particle size G_{max} can be perfectly predicted (mm)
e	Void ratio
$f(e)$	Void ratio function
G_{max}	Small strain shear modulus (MPa)
n	Elastic parameter from experimental data
p'	Mean effective stress (kPa)
p_a	Reference atmospheric pressure (kPa)
R	Roundness
S	Sphericity
t_a	Shear wave arrival time (s)
v_s	Velocity of travelling wave (m/s)
ρ_b	Bulk density (g/cm^3)
ρ	Regularity
σ_1-σ_3	Average stress difference (kPa)
σ_c	Average confining pressure (kPa)
ε_a	Axial strain increment (%)
ε_v	Volumetric strain increment (%)

REFERENCES

Been, K. and Jefferies, M.G. (1985). "A state parameter for sands." *Geotechnique*, **35**(2), 99-112.

Clayton, C.R., Theron, M., and Best, A.I. (2004). "The measurement of shear wave velocity using side-mounted bender elements in the triaxial apparatus." *Geotechnique*, **54**(7), 495-498. https://doi.org/10.1680/geot.2004.54.7.495

Cho, G.C., Dodds, J., and Santamarina, J.C. (2006). "Particle shape effects on packing density, stiffness and strength: natural and crushed sands." *Journal of Geotechnical and Geoenvironmental Engineering*, **132**(5), 591-602.

http://doi.org/10.1061/(ASCE)1090-0241(2006)132:5(591)

Gasparre, A., Hight, D.W., Coop, M.R., and Jardine, R.J. (2014). "The laboratory measurement and interpretation of small strain stiffness in stiff clay." *Geotechnique*, **57**(12), 942-953. https://doi.org/10.1680/geot.13.P.227

Hardin, B.O. (1985). "Crushing of soil particles." *Journal of Geotechnical and Geoenvironmental Engineering*, ASCE, **111**, 1177-1192. https://doi.org/10.1061/(ASCE)0733-9410(1985)111:10(1177)

Hardin, B.O. and Richart, F.E. (1963). "Elastic wave velocities in granular soils." *Journal of the Soil Mechanics and Foundations Division*, **89**(1), 33-65.

Jamiolkowski, M., Leroueil, S., and Lo Presti, D. (1991). "Design parameters from theory to practice." *Proceedings of International Conference on Geotechnical Engineering*, For coastal development, geo-coast, Yokohama Japan: Coastal Development Institute of Technology, 877-917.

Jamiolkowski, M., Lancellotta, R., and Lo Presti, D.C.F. (1995). "Remarks on the stiffness at small strains of six Italian clays." *Proceedings of International Symposium on Prefailure Deformation of Geomaterials*, Torino, 817-836.

Krumbein, W.C. and Sloss, L.L. (1963). *Stratigraphy and Sedimentation*. 2nd ed. San Francisco: Freeman and Company.

Lade, P.V., Yamamuro, J.A. and Bopp, P.A. (1996). "Significance of particle crushing in granular materials." *Journal of Geotechnical Engineering*, ASCE, **122**(4), 309-316. https://doi.org/10.1061/(ASCE)0733-9410(1996)122:4(309)

Li, W. and Senetakis, K. (2017). "Dynamic shear modulus of three reconstituted soils from panzhihua iron tailing dam." *Journal of GeoEngineering*, TGS, **12**(3), 129-135. http://dx.doi.org/10.6310/jog.2017.12(3).4

Nanda, S., Sivakumar, V., Donohue, S., and Graham S. (2017). "Small strain behavior and crushability of Ballyconnelly carbonate sand under monotonic and cyclic loading." *Canadian Geotechnical Journal*, **55**(7), 979-987. https://doi.org/10.1139/cgj-2016-0522

Okewale, I.A. and Coop, M.R. (2017). "A study of the effects of weathering on soils derived from decomposed volcanic rocks." *Engineering Geology*, **222**, 53-71. http://dx.doi.org/10.1016/j.enggeo.2017.03.014

Okewale, I.A. (2017). *Geotechnical and Geological Characterisation of Decomposed Volcanic Rocks from Hong Kong*. Ph.D. Dissertation, City University of Hong Kong.

Okewale, I.A. and Coop, M.R. (2018a). "On the effects of weathering on the compression behaviour of decomposed volcanic rocks." *TuniRock 2018*, Hammamet, Tunisia, 85-90.

Okewale, I.A. and Coop, M.R. (2018b). "Suitability of different approaches to analyze and predict the behaviour of decomposed volcanic rocks." *Journal of Geotechnical and Geoenvironmental Engineering*, ASCE, **144**(9), 1-14. http://doi.org/10.1061/(ASCE)GT.1943-5606.0001944

Okewale, I.A. (2019a). "Influence of fines on the compression behaviour of decomposed volcanic rocks." *International Journal of GeoEngineering*, **10**(4), 1-17. https://doi.org/10.1186/s40703-019-0101-y

Okewale, I.A. (2019b). "Effects of weathering on the stiffness characteristics and the small strain behaviour of decomposed volcanic rocks." *Journal of GeoEngineering*, TGS, **14**(2), 97-107. http://dx.doi.org/10.6310/jog.201906_14(2).5

Okewale, I.A. (2019c). "On the intrinsic behaviour of decomposed volcanic rocks." *Bulletin of Engineering Geology and the Environment*, 1-12. https://doi.org/10.1007/s10064-019-01643-7

Okewale, I.A. (2020). "Applicability of chemical indices to characterize weathering degrees in decomposed volcanic rocks." *Catena*, **189**, 1-13.

Payan, M., Khoshghalb, A., Senetakis, K., and Nasser, K. (2016). "Effect of particle shape and validity of Gmax models for sand: A critical review and a new expression." *Computer and Geotechnics*, **72**, 28-41. http://dx.doi.org/10.1016/j.compgeo.2015.11.003

Pennington, D.S., Nash, D.F.T., and Lings, M.L. (1997). "Anisotropy of G_o shear stiffness in Gault clay." *Geotechnique*, **47**(3), 391-398.

Rocchi, I. and Coop, M.R. (2015). "The effects of weathering on the physical and mechanical properties of a granitic saprolite." *Geotechnique*, **65**(6), 482-493. http://dx.doi.org/10.1680=geot.14.P.177

Rocchi, I., Okewale, I.A., and Coop, M.R. (2015). "The behaviour of Hong Kong volcanic saprolites in one-dimensional compression." *Volcanic Rocks and Soils*. Rotterdam: Balkema. 281-287. http://doi.org/10.1201/b18897-37

Saxena, S.K. and Reddy, K.R. (1989). "Dynamic moduli and damping ratios for Monterey No. 0 sand by resonant column tests." *Soils and Foundations*, **29**(2), 37-51.

Senetakis, K., Anastasiadis, A., and Pitilakis, K. (2012). "Small strain shear modulus and damping ratio of quartz and volcanic sands." *Geotechnical Testing Journal*, **35**(6). 964-80. GTJ20120073.

Vaggiani, G. and Atkinson, J.H. (1995). "Stiffness of fine-grained soil at very small strains." *Geotechnique*, **45**(2), 249-265. https://doi.org/10.1680/geot.1995.45.2.249